Effect of Symmetry Distortions on Photoelectron Selection Rules and Spectra on $Bi_2Sr_2CaCu_2O_{8+\delta}$

V. Arpiainen, M. Lindroos
Institute of Physics, Tampere University of Technology, P.O. Box 692, 33101 Tampere, Finland
(Dated: February 6, 2008)

We derive photoelectron selection rules along the glide plane in orthorhombic $Bi_2Sr_2CaCu_2O_{8+\delta}$ (Bi2212). These selection rules explain the reversed intensity behavior of the shadow and the main band of the material as a natural consequence of the variating representation of the final state as a function of $\boldsymbol{k}_\parallel$. Our one-step simulations strongly support the structural origin of the shadow band but we also introduce a scenario for detecting antiferromagnetic signatures in low doping.

PACS numbers: 79.60.-i, 71.18.+y, 74.72.Hs

Angle Resolved Ultraviolet Photoelectron Spectroscopy (ARUPS) is probably the most important tool to study the electronic structure of complex materials like the high T_c superconductors. It has been shown that matrix element effects must be taken into account in interpreting experimental data[1,2]. Using the one-step model of ARUPS and optical matrix elements, light has been shed on the strong variation of intensities due to the matrix element effects.[3,4,5] However, there are more strict rules dictating intensites in ARUPS, selection rules due to crystal symmetry. High resolution angular resolved photoemission measurements along high symmetry lines have been carried out recently to investigate the origin of the shadow bands in Bi2212[6,7]. Based on one-step computations, it was proposed that the shadow Fermi surface(FS) in Bi2212 has its origin in the orthorhombic (orth.) structure of the material.[6] In this study a need for selection rules emerged. In the orth. structure a mirror plane is broken into a glide plane. In this letter we give a group theoretical analysis for the selection rules along the glide plane and demonstrate the derived rules with one-step ARUPS simulations. We focus on Bi2212, but the derived selection rules may be applied to any cuprate superconductor with a similar structure.

The space group of the commonly used body-centered tetragonal(tetr.) structure for Bi2212 is number 139 in the International Tables for Chrystallography. In x-ray diffraction experiments an orth. structure has been found.[8] In this structure atoms are moved from their tetr. positions and the symmetry group is changed. The non-symmorphic space group of the orth. structure is the group number 66. The geometric structure of the superconducting cuprates may be described by a pile of planes of atoms. In the orth. structure the movements of the atoms from tetr. positions in the Cu-O-planes are small. Displacements are more clear in the Bi-O-plane, which is scetched in Fig. 1. Fig. 1(a) represents the tetr. Bi-O-plane and Fig. 1(b) the orth. Bi-O plane, where empty circles representing Bi-atoms and filled circles representing O-atoms are displaced. In the tetr. structure there are mirror planes corresponding to dashed lines in Fig. 1(a), but in the orth. structure only the mirror plane parallel to x axis remains. The mirror plane parallel to y axis is changed into a glide plane which is plotted with dash-dotted line in Fig. 1(b). This glide plane corresponds the glide-operation $\{\sigma_x|\mathbf{b}/2\}$, a reflection ($\sigma_x$ in the $x = 0$ plane) followed by a translation by half the primitive lattice vector in the y axis.

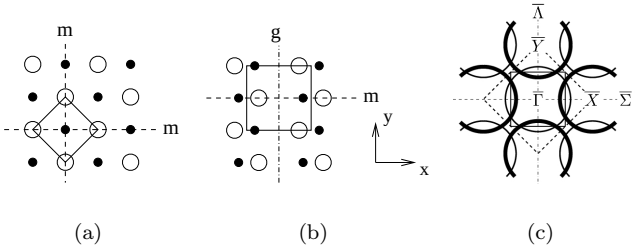

FIG. 1: Sketch of the positions of atoms in Bi2212. (a) Tetr. Bi-O layer, (b) orth. Bi-O layer, (c) Sketch of the Fermi surface.

The model FS of Bi2212 (only one sheet is shown for clarity) is sketched in Fig. 1(c). The figure shows the main band (FS of the tetr. structure) as thick circles and the shadow band as thin circles. In the figure the first tetr. Brillouin zone is approximately plotted with dashed line and the first orth. Brillouin zone with solid line. 2-dimensional $k_\parallel$-points of high symmetry $\bar{\Gamma}$,$\bar{X}$ and $\bar{Y}$ are also marked. The direction from $\bar{\Gamma}$ to $\bar{X}$ that is parallel to the mirror plane in real space is denoted by $\bar{\Sigma}$, and the direction from $\bar{\Gamma}$ to $\bar{Y}$ that is parallel to the glide plane by $\bar{\Lambda}$.[9] These directions are commonly known as the nodal directions.

The formula, based on the Fermi's golden rule, for the photocurrent by Feibelman and Eastman[10] can be manipulated into the form

$$I(E,\boldsymbol{k}_\parallel) \propto Im(\sum_{ij}\langle\psi^{(final)}_{f,\boldsymbol{k}_\parallel}|\mathbf{A}\cdot\mathbf{p}|\psi^{(initial)}_{i,\boldsymbol{k}_\parallel}\rangle \; G_{ij}\langle\psi^{(initial)}_{j,\boldsymbol{k}_\parallel}|\mathbf{A}\cdot\mathbf{p}|\psi^{(final)}_{f,\boldsymbol{k}_\parallel}\rangle), \quad (1)$$

where $\mathbf{A}$ is the vector potential of the incident photon and G_{ij} is a hole Green function. Photoemission selection rules arise from the symmetries of the initial (ψ_i)

and final (ψ_f) states and the dipole operator $\mathbf{A}\cdot\mathbf{p}$ in the matrix elements of Eq. 1. These selection rules are especially relevant along the mirror and glide planes, the directions $\overline{\Sigma}$ and $\overline{\Lambda}$ in Fig. 1(c). In the following analysis the dipole approximation is used, but the derivations are exact beoynd the approximation if the wave vector of the radiation lies in the symmetry plane that is under discussion.

In the mirror plane, since there is a well defined parity about the reflection in the plane, the selection rules can be derived by considering the parities of the components of the matrix element.[11] The transition is allowed if the entire dipole matrix element $\langle\psi_f|\mathbf{A}\cdot\mathbf{p}|\psi_i\rangle$ is even. With respect to reflection the final state with its momentum lying in the mirror plane is even. The operator $\mathbf{A}\cdot\mathbf{p}$ is even(odd) if the polarization is parallel(perpendicular) to the plane, which can be explained by considering parities of the initial state ψ_i and its derivative $\mathbf{A}\cdot\mathbf{p}\psi_i$, where $\boldsymbol{p}=-i\hbar\nabla$. The initial state at the Fermi level is similar to a Bloch sum of copper $d_{x^2-y^2}$ orbitals[20]. With respect to reflection this orbital and the Bloch sum with its momentum lying in the plane is odd. Thus, for photointensity to be nonzero the operator $\mathbf{A}\cdot\mathbf{p}$ must be odd and respectively polarization must be perpendicular to the mirror plane. This result is presented in combined form in table II. The even(identity) representation is denoted by Σ and the odd representation by Σ'.

Along the glide plane in the orth. structure the full machinery of the group theory has to be used. Photoemission selection rules due to glide plane have been considered previously by Pescia *et al.*[12] A good account of a more general procedure has been given by Bassani *et al.*[13]. The dipole matrix element $\langle\psi_f^{(\mu)}|(\mathbf{A}\cdot\mathbf{p})^{(\alpha)}|\psi_i^{(\nu)}\rangle$ will vanish if the irreducible representation(irrep) of the final state does not appear in the product of irreps of the initial state and the operator. The number of times it appears is given by[13]

$$c(\mathbf{k},\mu;\alpha;\mathbf{k},\nu) = \frac{1}{h_{\mathbf{k}}}\sum_{\{R_{\mathbf{k}}|\mathbf{f}\}}\chi^{(\mu)}(\{R_{\mathbf{k}}|\mathbf{f}\})^*\chi^{(\alpha)}(R_{\boldsymbol{k}})\chi^{(\nu)}(\{R_{\mathbf{k}}|\mathbf{f}\}), \quad (2)$$

where $\mathrm{h}_{\mathbf{k}}$ is the order(number of elements $\{R_{\mathbf{k}}|\mathbf{f}\}$) of the relevant little group for a particular $\boldsymbol{k}$-point in the first Brillouin zone. $\chi^{(\nu)}(\{R_{\mathbf{k}}|\mathbf{f}\})$ is the character of the little group irrep $\boldsymbol{D}^{(\nu)}(\{R_{\mathbf{k}}|\mathbf{f}\})$ for the initial state, $\chi^{(\mu)}(\{R_{\mathbf{k}}|\mathbf{f}\})$ the character of the irrep of the final state and $\chi^{(\alpha)}(R)$ is the character of the small point group representation $\boldsymbol{D}^{(\alpha)}(R_{\boldsymbol{k}})$ of the dipole operator. The little group of a particular k point contains operations $\{R|\mathbf{f}\}$ of the full space group that satisfy

$$\boldsymbol{R}\mathbf{k}=\mathbf{k}+\mathbf{G}, \quad (3)$$

i.e, leaving $\boldsymbol{k}$ unchanged. The small point group of $\mathbf{k}$ contains the rotational parts of the little group operations.

In the glide plane determined by direction $\overline{\Lambda}$ in Fig. 1(c), the little group(operations that keep $\boldsymbol{k}_\parallel=k_y\hat{\mathbf{k}}_\mathbf{y}$ and $\boldsymbol{k}_z$ unchanged) of the $\boldsymbol{k}$ vector in the plane contains two operations, identity operation $\{E|0\}$, and glide operation $\{\sigma_x|\mathbf{b}/2\}$. Both of the two operations form a class of their own and the eigenstates in the plane can be classified by two irreps. Character table for the little group is in table I.

TABLE I: Character table of the little group in plane $\bar{\Lambda}$. δ is $e^{-i\mathbf{k}\cdot\mathbf{b}/\mathbf{2}}$.

	E	$\{\sigma_x\|\mathbf{b}/2\}$
Λ	1	δ
Λ'	1	-δ

To proceed it has to be found out how to assign symmetry labels to particular final (and initial) states. The matching of the wave function at the surface of the sample rules out some of the possible final states. The final state in ARUPS is a time-reversed LEED state[10]. The irrep of this state may be obtained from the plane wave state $\psi_{\boldsymbol{k}_f}=e^{i(\mathbf{k}_f\cdot\mathbf{r})}$ that arrives to the detector[11]. The state is transformed under the glide operation according to

$$\begin{aligned} O_{\{\sigma_x|\mathbf{b}/2\}}\psi_{\mathbf{k}_f}(\mathbf{r}) &= \psi_{\mathbf{k}_f}(-x,y-b/2,z) \\ &= e^{i(k_{fy}(y-b/2)+k_{fz}z)} = e^{-ik_{fy}b/2}\psi_{\boldsymbol{k}_f}(\mathbf{r}) \\ &= e^{-i(k_y+G_y)b/2}\psi_{\boldsymbol{k}_f}(\mathbf{r}) = \delta e^{-in\pi}\psi_{\boldsymbol{k}_f}(\mathbf{r}), \end{aligned} \quad (4)$$

where k_y lies in the first Brillouin zone and $\boldsymbol{G}$ is a reciprocal lattice vector. The glide operation is represented by $\delta e^{-in\pi}$, where n is integer. The irrep of the final state is a function of the magnitude of the parallel component of its wavevector. It belongs to the irrep Λ in the 1.,3.,5.,... repeated Brillouin zone, and to the representation Λ' in the 2.,4.,6.,... zone. This fundamental result for ARUPS and glide plane was first shown by Pescia *et al.*[12] and has been exploited for Ni(100)-p(2x2)C[14] and TiO_2[15].

Operator $\mathbf{A}\cdot\mathbf{p}$ belongs to representation Λ of the small point group if polarization vector lies in the glide plane and to representation Λ' if it is perpendicular to the plane (parallel to x-axis). Photoemission selection rules follow from Eq. 2. They are presented in table II. In summary the initial state must belong to the same irrep as the final state if the polarization is parallel to the symmetry plane and to the other irrep if the polarization is perpendicular to the plane.

To finish the symmetry labels of the initial states forming FS have to be determined. As was discussed the movements of the atoms from the tetr. sites are very small in the copper-oxide layers and it can be assumed that the shape of the initial state is very close to the tetr. case, which can also be shown in the band structure calculations. Thus the initial state at FS belongs to the same irrep as a Bloch state of copper $\mathrm{d}_{x^2-y^2}$ orbitals. A Bloch sum of a Copper $d_{x^2-y^2}$ orbitals at a position

TABLE II: Dipole selection rules in the planes of high symmetry.

$\boldsymbol{k}_f$ in the mirror plane $\overline{\Sigma}$							
Repeated zone of $\boldsymbol{k}_{f\parallel}$	...	1.	2.	3.	4.	5.	...
Allowed final State irrep	...	Σ	Σ	Σ	Σ	Σ	...
Allowed initial state if $\boldsymbol{A} \perp \overline{\Sigma}$	...	Σ'	Σ'	Σ'	Σ'	Σ'	...
Allowed initial state if $\boldsymbol{A} \parallel \overline{\Sigma}$	...	Σ	Σ	Σ	Σ	Σ	...

$\boldsymbol{k}_f$ in the glide plane $\overline{\Lambda}$							
Repeated zone of $\boldsymbol{k}_{f\parallel}$	...	1.	2.	3.	4.	5.	...
Allowed final State irrep	...	Λ	Λ'	Λ	Λ'	Λ	...
Allowed initial state if $\boldsymbol{A} \perp \overline{\Lambda}$	...	Λ'	Λ	Λ'	Λ	Λ'	...
Allowed initial state if $\boldsymbol{A} \parallel \overline{\Lambda}$	...	Λ	Λ'	Λ	Λ'	Λ	...

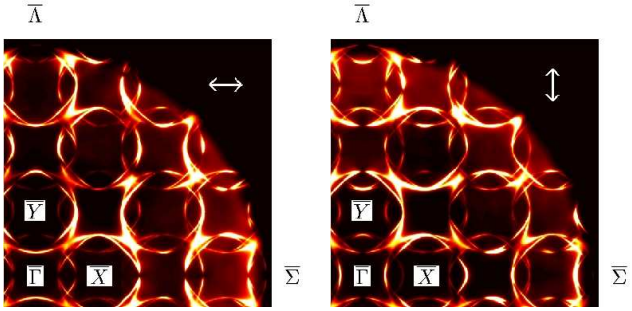

(a) (b)

FIG. 2: Bi2212 FS map. Normal incidence. (a) Polarization parallel to x-axis. (b) Polarization parallel to y-axis.

$\mathbf{d}_1 = 0.251\mathbf{a} + 0.5\mathbf{b} - 0.303\mathbf{c}$ is defined as

$$\phi_{\boldsymbol{d}_{x^2-y^2},Cu_1}(\boldsymbol{r}) = \sum_{\boldsymbol{\tau}_\nu} e^{i\mathbf{k}\cdot\boldsymbol{\tau}_\nu} \varphi_{d_{x^2-y^2}}(\mathbf{r} - \mathbf{d_1} - \boldsymbol{\tau}_\nu). \quad (5)$$

This can be decomposed into components belonging to different irreducible representations of the little group of $\boldsymbol{k}$ by[13]

$$\begin{aligned}\phi^{(\Lambda)}_{\boldsymbol{d}_{x^2-y^2}}(\boldsymbol{r}) =& \frac{1}{2}\left(\phi_{\boldsymbol{d}_{x^2-y^2},Cu_1}(\boldsymbol{r}) - e^{-i\mathbf{k}\cdot\mathbf{b}/2}\phi_{\boldsymbol{d}_{x^2-y^2},Cu_2}(\boldsymbol{r})\right),\\ \phi^{(\Lambda')}_{\boldsymbol{d}_{x^2-y^2}}(\boldsymbol{r}) =& \frac{1}{2}\left(\phi_{\boldsymbol{d}_{x^2-y^2},Cu_1}(\boldsymbol{r}) + e^{-i\mathbf{k}\cdot\mathbf{b}/2}\phi_{\boldsymbol{d}_{x^2-y^2},Cu_2}(\boldsymbol{r})\right),\end{aligned} \quad (6)$$

where $\phi_{\boldsymbol{d}_{x^2-y^2},Cu_2}(\boldsymbol{r})$ is a Bloch sum of an identical $d_{x^2-y^2}$ orbital at $\mathbf{d}_2 = -0.251\mathbf{a} + 0\mathbf{b} - 0.303\mathbf{c}$. These states can be pictured at Γ as bonding-antibonding states which have the opposite dispersion as a function of $\mathbf{k}_y$. $\phi^{(\Lambda')}_{d_{x^2-y^2}}$ is the bonding state with lower energy and $\phi^{(\Lambda)}_{d_{x^2-y^2}}$ the antibonding state. In the repeated zone scheme the state $\phi^{(\Lambda')}_{\boldsymbol{d}_{x^2-y^2}}$ represents the main band i.e. the band of the tetr. structure and the state $\phi^{(\Lambda)}_{\boldsymbol{d}_{x^2-y^2}}$ the shadow band.

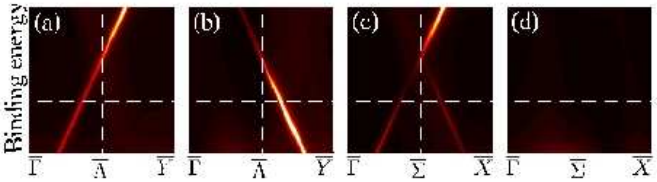

FIG. 3: Photoelectron spectra along high symmetry lines as a function of energy. (a) Along the glide plane, perpendicular polarization. (b) Along the glide plane, parallel polarization. (c) Along the mirror plane, parallel polarization. (d) Along the mirror plane, perpendicular polarization.

We have performed first-principles simulations of ARUPS spectra in Bi2212 using the one-step model of photoemission[16,17]. Fig. 2 shows the calculated FS of the orth. Bi2212 in the normal incidence setup. Double headed arrows indicate polarization of the incident light. Photon energy was 54 eV. Firstly we would like to remark that there seems to be no general correspondence between the intensitities of the main band and the shadow band. The effect of selection rules is seen in high symmetry directions $\overline{\Sigma}$ and $\overline{\Lambda}$. The FS map is probed at the fermi level and the initial state belongs to representation Λ' in the glide plane and to the representation Σ' in the mirror plane. In Fig. 2(a) polarization is parallel to the mirror plane and neither the shadow or the main is visible in $\overline{\Sigma}$-direction, whereas only the main band is visible in $\overline{\Lambda}$-direction. In Fig. 2(b) polarization is parallel to the glide plane and both of the bands are visible in $\overline{\Sigma}$-direction, whereas only the shadow band is visible in $\overline{\Lambda}$-direction. This phenomena has also been shown experimentally[6,7]. The strange behavior of the shadow band follows from the variating irrep of the final state in the consequent Brillouin zones.

Fig. 3 shows photointensity as a function of binding energy and $k_\parallel$. Calculations were performed within the normal incidence setup, photon energy was 40 eV. The Fermi function was ignored. Fig. 3(a) and 3(b) show results along the glide plane with polarization perpendicular to the plane(Fig.(a), main band visible) and parallel to the plane(Fig.(b), shadow band visible). Fig. 3(c) and 3(d) show the corresponding results along the mirror plane. Along the glide plane the main and the shadow band seem to give continuous intencity as a function of $\boldsymbol{k}_\parallel$ even when crossing the zone barrier. This can again be explained with table II. When an initial state band crosses the zone barrier it can be mapped to the other band in the first Brillouin zone and it's irrep, as the irrep of the final state, will change.

Furthermore, there is one surprising consequence of the selection rule due to glide plane. As this rule states the final states for the shadow and the main band must belong to a different irrep along $\overline{\Lambda}$-line. Consequently, when pic-

turing the band structure, the final state for the shadow band cannot be an umklapp of the final state for the main band, but on the contrary it must lie in some other available band with fixed final state energy. This means that the intensities of the bands varie e.g. as a function of photon energy in an uncorrelated way, which can also be seen as a function of binding energy in Fig.3(a) and 3(c). Actually because of the fact that the width (due to Σ_f'' and $\boldsymbol{k}_\perp$ dispersion[18]) of the final state is relatively large, both the main and the shadow band can be observed with the same single photon energy.

Available experimental data are consistent with our predicted intensities due to structural distortions, but we also point out that the intensity variation along the glide plane strongly masks any weak sign of antiferromagnetism(AFM) induced spectral features. We have modelled the molecular field of the AFM interaction with planar ordering, which is known to exist in La_2CuO_{4-y}[19], by an *ad hoc* parameter u on copper sites. Our computations reveal that, to produce shadow bands in ARUPS by AFM, relatively large u has to be used.

But there is one interesting possiblitity. If both the structural and the AFM interactions were present, as must be with low doping, the selection rules would change again. The correct magnetic group should be determined, but because the specification of the magnetic moments in Bi2212 is not available and because of limitations of our program code, we can only discuss the AFM selection rules qualitatively. While maintaining the reflection symmetry the *ad hoc* planar ordering breaks the glide symmetry, and, consequently, the derived selection rules along the glide plane would be no longer valid. In practice, this would mean that, in those high symmetry directions where the structural distortions forbid intensity, there could exist signatures of the FS due to the AFM interaction. In Fig. 4 we have calculated the effect of the AFM on ARUPS spectra. The magnitude of u was 0.9 eV, which induces an energy gap of the same magnitude. In contrast to Fig. 3, along the glide plane (Fig. 4a and Fig. 4b), there are no longer strict selection rules for the polarization, and the main and the shadow band are, though weakly, visible with both polarizations. Along the mirror plane [Figs. 4c and 4d] the selection rules remain strict. We thus urge experimetalists to focus some measurements with high flux and precise polarizations to look possible signatures of AFM features. A development of the AFM gap with lowered doping and maybe other signatures of the AFM may be seen in this way.

We have shown that structural modifications in Bi2212 from a body centered tetragonal lattice to a base-centered orthorhombic lattice change selection rules in ARUPS along the high symmetry lines. Because of the glide plane in orthorhombic structure, it turns out that the irreducible representation of the final state changes alternatively in the repeated zone scheme of $\boldsymbol{k}_\parallel$ space. With fixed polarization this yields opposite intensity behaviour for the main and the shadow FS in the adjacent Brillouin zones. The calculated FS is consistent with available experimental data, which is strong evidence against the antiferromagnetic scenario, but a possibility of detecting AFM features in low doping is proposed.

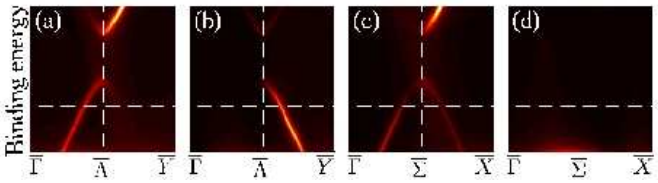

FIG. 4: Photoelectron spectra along the high symmetry lines as a function of energy, including AFM-effect, $u = 0.9$ eV. (a) Along the glide plane, perpendicular polarization. (b) Along the glide plane, parallel polarization, (c) Along the mirror plane, perpendicular polarization, (d) Along the mirror plane, parallel polarization.

Acknowledgments

This work is funded from the Academy of Finland and benefited from the Institute of Advanced Computing (IAC), Tampere.

[1] A. Bansil and M. Lindroos, Phys. Rev. Lett. **83**, 5154 (1999).
[2] M. C. Asensio, J. Avila, L. Roca, A. Tejeda, G. D. Gu, M. Lindroos, R. S. Markiewicz, and A. Bansil, Phys. Rev. B **67**, 14519 (2003).
[3] M. Lindroos, S. Sahrakorpi, and A. Bansil, Phys. Rev. B **65**, 54514 (2002).
[4] S. Sahrakorpi, M. Lindroos, and A. Bansil, Phys. Rev. B **68**, 54522 (2003).
[5] A. Bansil, M. Lindroos, S. Sahrakorpi, and R. S. Markiewicz, New J. Phys. **7**, 140 (2005).
[6] A. Mans, I. Santoso, Y. Huang, W. K. Siu, S. Tavaddod, V. Arpiainen, M. Lindroos, H. Berger, V. N. Strocov, M. Shi, et al., Phys. Rev. Lett. **96**, 107007 (2006).
[7] M. Izquierdo, J. Avila, L. Roca, G. Gu, and M. C. Asensio, Phys. Rev. B **72**, 174517 (2005).
[8] P. A. Miles, S. J. Kennedy, G. J. McIntyre, G. D. Gu, G. J. Russel, and N. Koshizuka, Physica C **294**, 275 (1998).
[9] G. C. Fletcher, *The Electron Band Theory of Solids* (N-H P. Co., 1971).
[10] P. J. Feibelman and D. E. Eastman, Phys. Rev. B **10**, 4932 (1974).
[11] J. Hermanson, Solid State Commun. **22**, 9 (1977).
[12] D. Pescia, A. Law, M. Johnson, and H. Hughes, Solid State Commun. **56**, 809 (1985).
[13] F. Bassani and G. P. Parravicini, *Electronic States and*

Optical Transitions in Solids (Pergamon press, 1975).
[14] K. C. Prince, M. Surman, T. Lindner, and A. M. Bradshaw, Solid State Commun. **59**, 71 (1986).
[15] P. J. Hardman, G. N. Raikar, C. A. Muryn, G. van der Laan, P. L. Wincott, G. Thornton, D. Bullett, and P. Dale, Phys. Rev. B **49**, 7170 (1994).
[16] J. B. Pendry, Surf. Sci. **57**, 679 (1976).
[17] A. Bansil and M. Lindroos, J. Phys. Chem. Solids **59**, 1879 (1998).
[18] S. Sahrakorpi, M. Lindroos, R. S. Markiewicz, and A. Bansil, Phys. Rev. Lett. **95**, 157601 (2005).
[19] D. Vaknin, S. K. Sinha, D. E. Moncton, D. C. Johnston, and J. M. Newsam, Phys. Rev. Lett. **58**, 2802 (1987).
[20] In the rotated orthorhombic coordinate system of Fig. 1 these are d_{xy} orbitals